Appl. Phys. A (2016) 122:925
DOI 10.1007/s00339-016-0453-5

Applied Physics A
Materials Science & Processing

Synthesis and thermal properties of new bionanofluids containing gold nanoparticles

J. L. Jiménez-Pérez[1] · G. López Gamboa[1,2] · R. Gutiérrez Fuentes[3] · J. F. Sánchez Ramírez[4] · Z. N. Correa Pacheco[5] · V. E. López-y-López[4] · L. Tepech-Carrillo[6]

Received: 26 January 2016 / Accepted: 20 September 2016 / Published online: 30 September 2016

Abstract New bionanofluids containing Au nanoparticles with different concentrations were prepared by chemical reduction method. The nanoparticles were mixed with biodiesel from soybean prepared using alkaline catalysts. Thermal properties of biodiesel containing Au nanoparticles with different volume percentage concentrations were measured by mismatched dual-beam mode thermal lens technique in order to measure the effect of the presence of nanoparticles ($\varphi = 13.3$ nm) on the bionanofluids thermal diffusivity. The characteristic time constant of the transient thermal lens was estimated by fitting the experimental data to the theoretical expression for transient thermal lens. The thermal diffusivity of the bionanofluids (biodiesel containing Au nanoparticles) seems to be strongly dependent on the presence of nanoparticles. It was observed an increase in the thermal diffusivity when volume percentage of nanoparticles increased. A possible explanation for such high thermal diffusivity of the biodiesel with Au nanoparticles is given. UV–Vis spectroscopy and TEM microscopy techniques were used to characterize the bionanofluids.

✉ J. L. Jiménez-Pérez
jimenezp@fis.cinvestav.mx

[1] UPIITA-Instituto Politécnico Nacional, Av. Instituto Politécnico Nacional 2580, Barrió Laguna Ticomán, 07340 Mexico, D.F., Mexico

[2] Universidad Politécnica del Valle de Toluca (UPVT), km 5.7 Carretera Almoloya de Juárez, Santiaguito Tlalcilalcali, C.P. 50904, Mexico, Estado de México, Mexico

[3] CINVESTAV-IPN, Unidad Mérida, Antigua carretera a Progreso Km 6, Cordemex, 97310 Mérida, Yucatán, Mexico

[4] CIBA-Instituto Politécnico Nacional, San Juan Molino Km 1.5 de la Carretera Estatal Sta. Inés Tecuexcomac-Tepetitla, 90700 Mexico, Tlaxcala, Mexico

[5] Instituto Politécnico Nacional-Centro de Desarrollo de Productos Bióticos, Carretera Yautepec–Jojutla, km 6.8, San Isidro, Yautepec, C.P. 62730, Mexico, Morelos, Mexico

[6] Escuela de Ciencias, Universidad Autónoma Benito Juárez de Oaxaca, C.P. 68120 Oaxaca de Juárez, Oaxaca, Mexico

1 Introduction

There is a need for alternative energy sources to petroleum-based fuels due to the depletion of the world's petroleum reserves, global warming and environmental concerns. Biodiesel is a clean and renewable fuel, which is considered the best substitution for diesel fuel [1]. Soybean is a major crop throughout much of North America, South America and Asia. The USA is the world's greatest soybean producer with approximately 32 % of the total production followed by Brazil with 28 %. Soybeans contain approximately 18–20 % oil compared to other oilseed crops such as canola (40 %) and sunflower (43 %) [2]. Soybean oil is currently a major feedstock for production of biodiesel (NBB). The most common method of biodiesel production is a reaction of vegetable oils or animal fats with methanol or ethanol in the presence of sodium hydroxide (which acts as a catalyst). The transesterification reaction yields methyl or ethyl esters (biodiesel) and a byproduct of glycerin [3]. In addition to biodiesel production, soybeans can be used to produce ethanol. Soybean hulls contain significant amount of carbohydrate for ethanol production, and producers prefer to use soybean hulls for animal feeding because of its high protein content [4]. Although, biodiesel is usually seed as a blend with petrodiesel at varying ratios, it can also be used to fuel compression ignition engines alone. The results of engine emission tests showed that use of biodiesel alone produced

less emissions of CO, HC, NOx and smoke than petrodiesel [5].

Recent advances in nanomaterials and nanotechnology have led to the development of new class of heat-transfer fluids containing nanometer-sized particles called nanoparticles (NPs) typically made of carbon nanotubes, metals or oxides. Nanofluids are suspensions of nanoparticles with average sizes below 100 nm in a base fluid such as water, ethylene glycol and oil. Compared with the base fluid, nanofluids have distinctive properties that make them attractive in many applications such as pharmaceutical processes, transportation industry, thermal management of electronics, fuel cells, boiler flux gas temperature reduction and heat exchangers. [6, 7].

In the last years, photothermal techniques have been used in a wide range of scientific areas to study several of materials physics including transport and thermal properties. Regarding thermal properties, the thermal lens (TL) technique is employed for thermal characterization of several materials by measuring their thermal diffusivity (D). A TL occurs when energy absorbed from a Gaussian beam produces local heating within the absorbing medium around the beam axis. In such experiment, the sample is exposed to a laser beam, which has a Gaussian profile and it causes excitation of the molecules along beam path. Thermal relaxation of the excited molecules dissipates heat into the surroundings, thereby creating a temperature distribution that produces a refractive index gradient normal to beam axis within the medium. This acts as a diverging (negative) or convergent (positive) lens so called as TL [8]. This TL technique is a high-sensitivity and nondestructive optical technique and thermal properties of transparent samples with an enhanced accuracy, for solid samples and fluids. Recently the TL technique was used to measure the thermal diffusivity of nanofluids with different solvents, being observed that the thermal diffusivity values of the base fluids was enhanced by the presence of gold nanoparticles [9]. TL was successfully used to measure the thermal diffusivity of diverse vegetable oils [10]. In this work, thermal diffusivities of soybean biodiesel containing nanoparticles of Au using a dual-beam mismatched-mode TL experimental setup is reported.

2 Theory

The theoretical treatment of the thermal lens effect takes into account the spherical aberration of the thermal lens and considers the whole optical path length change with temperature. Shen et al. developed the infinitive aberrant model for the mode-mismatched configuration, using the two boundary conditions $\Delta T\,(r, 0) = 0$, $(r < \infty)$ and $\Delta T\,(\infty, t) = 0$ $(t > 0)$, the temporal evolution of the temperature profile $\Delta T\,(r, t)$ induced by the TL in the sample is given by Shen et al. [8].

The temperature increase, which carries a Gaussian profile, induces a slight distortion in the probe beam wave front that can be associated with the change in the refractive index of the sample with respect to the axis of beam, as follows:

$$\frac{\Phi\lambda_{\mathrm{p}}}{2\pi} = l_0\left(\frac{\mathrm{d}n}{\mathrm{d}T}\right)_{\mathrm{p}}[\Delta T(r,t) - \Delta T(0,t)] \tag{1}$$

In which Φ is the phase shift induced when the probe beam passes through the TL, λ_{p} is the probe beam wavelength, l_0 is the sample thickness and $(\mathrm{d}n/\mathrm{d}T)_{\mathrm{p}}$ is the temperature dependence of the refractive index of the sample. Finally, using the Fresnell diffraction theory, the probe beam intensity at the detector plane can be written as an analytical expression for absolute determination of the thermo-optical properties of the sample, as [8]:

$$I(t) = I(0)\left[1 - \frac{\theta}{2}\tan^{-1}\left(\frac{2mV}{\left[(1+2m)^2 + V^2\right]\frac{t_{\mathrm{c}}}{2t} + 1 + 2m + V^2}\right)\right]^2 \tag{2}$$

In Eq. (1), $I\,(0)$ is the signal intensity when either t or θ is zero; θ is proportional to the induced phase shift difference in the probe beam after it passes by the heated area of the sample and the equation for θ is [8]:

$$\theta = -\frac{P_{\mathrm{e}}AL}{k\lambda_{\mathrm{p}}}\frac{\mathrm{d}n}{\mathrm{d}T} \tag{3}$$

where P_{e} (40 mW) is the incident power, A (cm^{-1}) is the sample's absorption coefficient, λ_{p} (632.8 nm) is the wavelength of probe beam, L (1 cm) is the cuvette thickness, k (W/K cm) is the thermal conductivity, $\mathrm{d}n/\mathrm{d}T$ (K^{-1}) is the refractive index temperature coefficient and t_{c} is the so-called characteristic time constant of the TL effect's formation, which is defined as $t_{\mathrm{c}} = \omega_{\mathrm{e}}^2/4\ D$ with $\omega_{\mathrm{e}} = 3.98 \pm 0.02 \times 10^{-3}$ cm the spot size of the excitation laser beam at the sample; D is the thermal diffusivity ($D = k/\rho c$, where k is the thermal conductivity, ρ is the density and c is the specific heat of the nanofluid); $m = (w_{1\mathrm{p}}/w_{\mathrm{e}})^2$, with $w_{1\mathrm{p}}$ (cm) being the probe beam's radius in the sample position and $V = Z_1/Z_{\mathrm{c}}$, with Z_1 (cm) being the distance between the minimum beam waist and the sample position; $Z_{\mathrm{c}} = \pi\,\omega_{\mathrm{op}}^2/\lambda_{\mathrm{p}}$, with ω_{op} (cm) being the minimum probe beam radius; the values of m and V are constants.

Prior to the experiments on nanofluids, the TL setup was calibrated using distilled water as a sample, resulting in the following values: $m = 22.54 \pm 0.01$, $V = 0.62 \pm 0.01$.

3 Materials and methods

3.1 Production of biodiesel by transesterification of refined soy oil

The reaction of transesterification was carried out in a 250-ml Erlenmeyer flask containing 452 g of soy oil. This was conducted at 45 °C, under magnetic stirring at 250 rpm with an oil (4.80 mol) to methanol (1.60 mol) ratio constant of 1:3. Sodium hydroxide solution (1.0 %, w/w) was used as catalyst. The catalyst was dissolved into methanol according to the oil to alcohol (1:3, mol:mol). The oil was heated up to reaction temperature in Erlenmeyer flask, and once the alkali got dissolved, the alcohol–alkali mixture was added to the oil, and the reaction transesterification was allowed for 60 min. This sample was allowed to settle overnight in a separating funnel by gravity, settling into a clear, golden liquid biodiesel on top with the light brown glycerol at the bottom. On the second day, the glycerol was drained off from the bottom of the separating funnel. The raw biodiesel was washed with water three times to remove the unreacted catalysis and glycerol. To get a pure biodiesel, this was purified in a rotary evaporator to remove any excess methanol.

3.2 Preparation of metallic bionanofluids

In order to obtain biodiesel containing gold nanoparticles, the gold nanoparticles were first synthesized by borohydride reduction of aqueous $HAuCl_4{\cdot}3H_2O$ solution (0.0013 M) in a manner analogous described by Patil et al. [11]. This results in a clear reddish aqueous colloidal solution containing gold nanoparticles of 3.2 nm average size. To 10 ml of the gold colloidal solution thus prepared, solution of octadecylamine (ODA, 0.013 mmol) in biodiesel (10 ml) of soy oil was added to yield immiscible layers of the colorless organic solution on top of the aqueous solution. Vigorous shaking of the test tube resulted in transfer of the gold colloidal nanoparticles into the biodiesel, and this was observed by the red coloration on the biodiesel—and a corresponding loss of color of the aqueous phase when the two layers separated out. The process of washing with ethanol removes uncoordinated ODA molecules from biodiesel. Finally, the bionanofluid (which are mixture of gold nanoparticles in a biodiesel) was placed in a quartz cuvette of 1 cm thick for the optical and thermal measurement. Bionanofluids with percentage by volume of gold nanoparticles were 0.027, 0.013, 0.0087, 0.0067, 0.0054 and 0.0045 vol/%. The metallic bionanofluids were stable for months without significant changes in the spectral pattern. All the experiments were performed at room temperature and subjected to ultrasonic processing prior to each measurement.

3.3 Characterization

A Shimadzu UV-3101PC double-beam spectrophotometer with slit wavelength of 2 nm and light path length of 1 cm was used to record the absorption spectra of the bionanofluids. Particle sizes and size distribution were evaluated by transmission electron microscopy (TEM), using JEOL-JEM200 microscope. For TEM observations, a drop of aqueous colloidal solution of gold nanoparticles was spread on a carbon-coated copper microgrid and dried subsequently in vacuum.

4 Results and discussion

Figure 1 shows the morphology of the nanoparticles. In Fig. 1a, the TEM image of the gold nanoparticles, which mean diameter of 13.3 nm, is observed. Au nanoparticles are spherical in shape. The histogram for nanoparticle distribution is shown in Fig. 1b.

The optical absorption spectrum of biodiesel oil had a peak absorption peak around 230 nm and two bands at 270 and 285 nm in the UV region (Fig. 2). The typical optical absorption spectrum of the gold nanoparticles solutions shows a peak absorption band at 360 nm and a broad band around 523 nm. The absorption peak of lower energy is generally assigned to the surface plasmon resonance (SPR) of spherical gold nanoparticle [12].The blends of biodiesel oil and gold nanoparticles are intermediate between the two components with sharp peaks at 344 nm for bionanofluids with 0.0045 vol/% of Au NPs, 350 nm with 0.0054 vol/% of Au NPs, 351 nm with 0.0067 vol/% of Au NPs, 352 nm with 0.0087 vol/% of Au NPs, 353 nm with 0.013 vol/% of Au NPs, 356 nm with 0.027 vol/% of Au NPs and broad bands at around 523 nm.

From this figure, we observe that with the increase in Au NPs concentration in the bionanofluids, the intensity of the peak around 523 nm increased. This is not surprising, since a large number of nanoparticles provide higher surface for surface plasmon resonance.

Figure 3 shows a typical transient thermal lens signal evolution for soybean biodiesel with an Au nanoparticle concentration of 0.013 %. The experimental TL signal is represented by open circles, while the solid line corresponds to the best fit of Eq. (1) to experimental data, leaving $\theta = 3.9 \pm 0.01 \times 10^{-2}$ and $t_c = 19.5 \pm 0.3 \times 10^{-4}$ s as adjustable parameters and $D = (22.9 \pm 0.3) \times 10^{-4}$ cm^2 s^{-1} as best fitting parameter values. In a similar

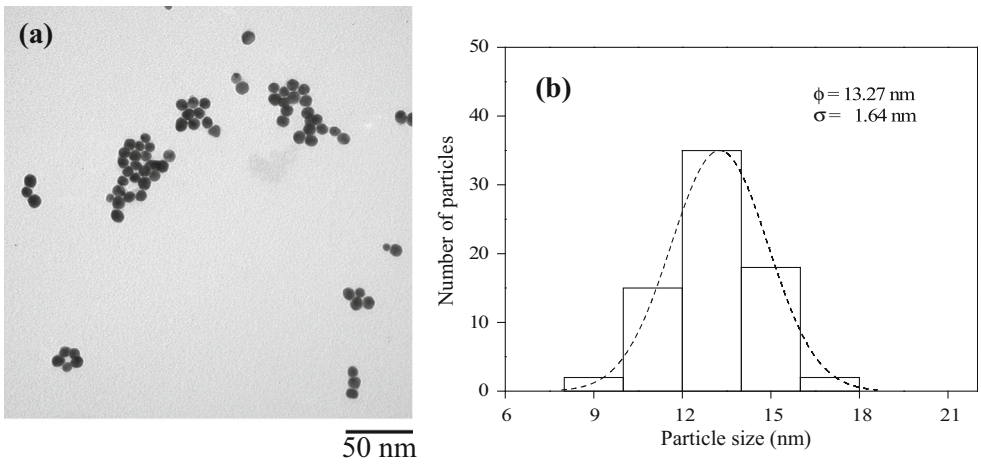

Fig. 1 **a** TEM image and **b** nanoparticles size of histogram of Au particles with a mean size of 13.3 nm

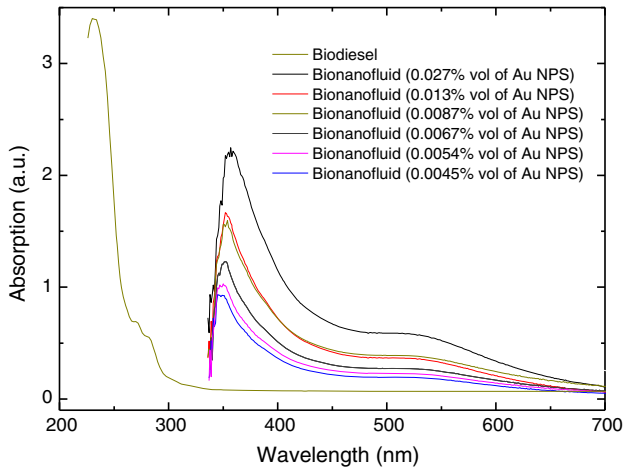

Fig. 2 UV–Vis absorption spectra for: biodiesel and bionanofluids for different concentrations

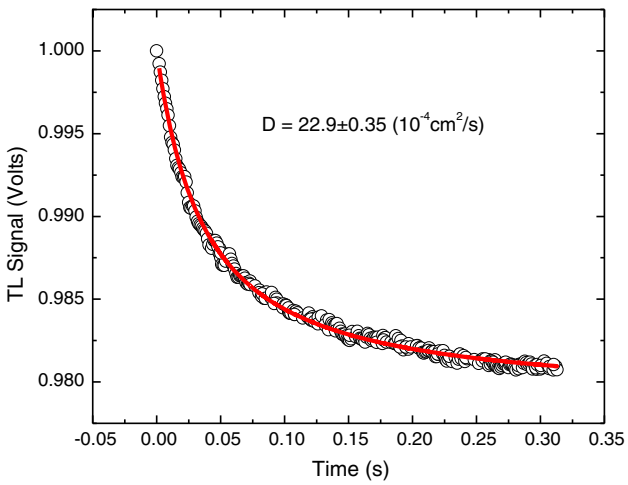

Fig. 3 Thermal lens signal of the Au/biodiesel (0.013 vol%); *empty circles* (o) represent experimental points and the *red line* is the best fit with Eq. (1)

way, from the best fit of Eq. (2) to the experimental data, the thermal diffusivities of the other nanofluid samples were obtained at room temperature: $D = (24.1 \pm 0.5) \times 10^{-4}$ cm^2 s^{-1}, $D = (20.9 \pm 0.4) \times 10^{-4}$ cm^2 s^{-1}, $D = (19.9 \pm 0.3) \times 10^{-4}$ cm^2 s^{-1}, $D = (18.2 \pm 0.3) \times 10^{-4}$ cm^2 s^{-1} and $D = (17.3 \pm 0.5) \times 10^{-4}$ cm^2 s^{-1}, for samples with Au nanoparticle concentrations 0.027, 0.0087, 0.0067, 0.0054 and 0.0045 %, respectively. The thermal diffusivity values obtained for biodiesel with gold nanoparticles are (slightly) higher than the one of pure biodiesel, $16.3 \pm 0.2 \times 10^{-4}$ cm^2 s^{-1} (the reported value in the literature for pure biodiesel is 14.0×10^{-4} cm^2 s^{-1} [13–15]). The increment in the thermal diffusivity goes from 6 to 47 % for the different Au nanoparticle concentrations (Table 1). There is a significant increase in thermal diffusivity with increasing Au nanoparticle concentration, for all measured suspensions.

The observed increase in the thermal diffusivity can be attributed to the great thermal diffusivity of the Au nanoparticles contained in the biodiesel (oil). Many authors have reported that the enhancement in the thermal diffusivity of oleic acid is attributed to the thermal diffusivity of individual carbon nanotubes for suspensions with 0.5 % with an increase in thermal diffusivity of 20 % [7]. On the other hand, for 1.0 vol% nanotubes, the increase was 136 % [16]. Moreover, an enhancement of 70 % for 0.1 wt% of nanodiamonds in mineral oil is reported by Taha-Tijerina et al. [17].

In the literature, authors have pointed out many causes for the thermal increase in nanofluids. It is possible to list some physical reasons to explain this improvement in the heat transfer performance of nanofluids as follows: (1) The suspended nanoparticles increase the surface area and the heat capacity of fluid; (2) the suspended nanoparticles increase the effective thermal conductivity of the fluid; (3)

Table 1 Dependence of the thermal diffusivity and other fitting parameter values of bionanofluids on the concentration of gold nanoparticles

Bionanofluids (vol% of Au NPs)	t_c (10^{-4}s)	θ ($\times 10^{-2}$)	D (10^{-4} cm^2/s)	Increase (%)
0.027	18.2 ± 0.4	4.1 ± 0.02	24.1 ± 0.5	47
0.013	19.5 ± 0.3	3.9 ± 0.01	22.9 ± 0.3	36
0.0087	21.3 ± 0.4	2.7 ± 0.02	20.9 ± 0.4	28
0.0067	22.4 ± 0.4	2.2 ± 0.01	19.9 ± 0.3	22
0.0054	24.5 ± 0.4	2.8 ± 0.01	18.2 ± 0.3	12
0.0045	25.9 ± 0.1	2.4 ± 0.01	17.3 ± 0.5	6
Soybean biodiesel	27.4 ± 0.4	3.9 ± 0.01	16.3 ± 0.2	Pure biodiesel

the interaction and collision among particles, fluid and the flow passage surface are intensified; (4) the mixing fluctuation and the turbulence of the fluid are intensified; and (5) the dispersion of nanoparticles slightly modifies the transverse temperature gradient of the fluid [7].

As mentioned in the previous paragraph, there are many causes for the temperature increase in nanofluids with many parameters that affect the thermal conductivity. However, the traditional models available are not able to account all the differences. The classical Maxwell [18] equation is used for predicting thermal conductivity for micro-sized suspension; Bruggemans [19] equation is used for high volume fraction, whereas Hamilton and Crosser [20] include the effect of shape of nanoparticle. The Maxwell equation was modified by Yu and Choi [21] to include the effect of liquid layering and a model with sum of Maxwell, and terms accounting Brownian motion were presented by Koo and Kleinsteuer [22]. All the equations available in the literature are inefficient to account all the parameters affecting the thermal conductivity of nanofluids. In this paper, a new model is under study for thermal conductivity estimation of nanofluids prepared with vegetable oil. The combined effect of all the factors of Au such as the size, diameter of the particles, thermal conductivity, volume fraction and base fluids has been studied. In a previously published paper [23], the Kumar model [24] was used in order to determine the thermal diffusivity of biodiesel C4 incorporating Au nanoparticles and the effective enhancement. However, the model was valid only for smaller concentrations. Therefore, the new theoretical model is being developed in order to explain the nonlinear behavior and diffusion mechanisms of metallic nanoparticles incorporated into biodiesel due to anomalous effects.

5 Conclusions

The thermal lens has been used to determine the thermal diffusivity dependence with Au nanoparticles concentration suspended in soybean biodiesel. 6–47 percentage of enhancement relative to pure biodiesel was observed for bionanofluids (biodiesel containing Au nanoparticles). It is concluded that the thermal properties and good dispersion ability of Au nanoparticles contributed to the significant improvement in the effective thermal diffusivity of the bionanofluids analyzed.

Acknowledgments We would like to thank CONACYT, COFAA and CGPI-IPN, México.

References

1. S.P. Singh, Renew. Sustain. Energy Rev. **14**, 200 (2010)
2. D.R. Berglund, K. McKay, J. Knodel, Canola Production, North Dakota State University, A-686 (2007)
3. https://cropwatch.unl.edu/bioenergy/soybeans
4. J.R. Mielenz, J.S. Bardsley, C.E. Wyman, Bioresour. Technol. **100**, 3532 (2009)
5. D.H. Qi, L.M. Geng, H. Chen, Y.Z. Bian, J. Liu, X.C. Ren, Renew. Energy **34**, 2706 (2009)
6. W.J. Minkowycz, E.M. Sparrow, J.P. Abraham, *Nanoparticle Heat Transfer and Fluid Flow* (CRC Press, Boca Raton, USA, 2012), pp. 25–67
7. A.J. de Freitas Cabral, C. Aparecida Furtado, C. Fantini, P. Alcantara Jr., J. Nano Res. **21**, 125 (2013)
8. J. Shen, R.D. Lowe, R.D. Snook, Chem. Phys. **165**, 385 (1992)
9. J.L. Jiménez Pérez, A. Cruz Orea, J.F. Sánchez Ramírez, F. Sánchez Sinencio, L. Martínez Pérez, G.A. López Muñoz, Int. J. Thermophys. **30**, 1227 (2009)
10. J.L. Jiménez Pérez, A. Cruz-Orea, P. Lomelí Mejia, R. Gutierrez Fuentes, Int. J. Thermophys. **30**, 1396 (2009)
11. V. Patil, R.B. Malvankar, M. Sastry, Langmuir **15**, 8197 (1999)
12. E. Shahriari, W.M. Mat Yunus, R. Zamiri, J. Eur. Opt. Soc. Rap. Public **8**, 13026 (2013)
13. M. Ventura, E. Simionatto, L.H.C. Andrade, E.L. Simionatto, D. Riva, S.M. Lima, Fuel **103**, 506 (2013)
14. S.M. Lima, M.S. Figueiredo, L.H.C. Andrade, A.R.L. Caíres, S.L. Oliveira, F. Aristone, Appl. Opt. **48**, 5728 (2009)
15. R.F. Souza, M.A.R.C. Alencar, C.M. Nascimento, M.G.A. da Silva, M.R. Meneghetti, J.M. Hickmann, Proc. SPIE **6323**, 63231T (2006)
16. S. Shaikh, K. Lafdi, R. Ponnappan, J. Appl. Phys. **101**, 064302 (2007)
17. J. Taha-Tijerina, T. Narayanan, C. Sekhar, K. Lozano, M. Chipara, P. Ajayan, Appl. Mater. Interfaces **6**, 4778 (2014)
18. J.C. Maxwell, *A Treatise on Electricity and Magnetism* (Oxford University Press, Cambridge, 1904)

19. D.A.G. Bruggeman, Ann. Phys. **416**, 636 (1935)
20. R.L. Hamilton, O.K. Crosser, Ind. Eng. Chem. Fundam. **1**, 187 (1962)
21. S.U.S. Choi, W. Yu, J. Nanopart. Res. **5**, 167 (2003)
22. J. Koo, C. Kleinstreuer, J. Nanopart. Res. **6**, 577 (2004)
23. J.L. Jiménez-Pérez, R.G. Fuentes, Z.N. Correa Pacheco, J. Tanori Cordova, A. Cruz Orea, G. López Gamboa, Int. J. Thermophys. **36**, 1086–1092 (2015)
24. D.H. Kumar, H.E. Patel, V.R. Rajeev Kumar, T. Sundarajan, T. Pradeeep, S.K. Das, Phys. Rev. Lett. **93**, 1–144301 (2004)